—Original Article—

The CDKN1B-RB1-E2F1 pathway protects mouse spermatogonial stem cells from genomic damage

Takashi TANAKA[1], Mito KANATSU-SHINOHARA[1, 2] and Takashi SHINOHARA[1]

[1)]*Department of Molecular Genetics, Graduate School of Medicine, Kyoto University, Kyoto 606-8501, Japan*
[2)]*Japan Science and Technology Agency, PRESTO, Kyoto 606-8501, Japan*

Abstract. Spermatogonial stem cells (SSCs) undergo self-renewal divisions to provide the foundation for spermatogenesis. Although *Rb1* deficiency is reportedly essential for SSC self-renewal, its mechanism has remained unknown. Here we report that *Rb1* is critical for cell cycle progression and protection of SSCs from DNA double-strand breaks (DSBs). Cultured SSCs depleted of *Cdkn1b* proliferated poorly and showed diminished expression of CDK4 and RB1, thereby leading to hypophosphorylation of RB1. *Rb1* deficiency induced cell cycle arrest and apoptosis in cultured SSCs, which expressed markers for DNA DSBs. This DNA damage is caused by increased E2F1 activity, the depletion of which decreased DNA DSBs caused by *Rb1* deficiency. Depletion of *Cdkn1a* and *Bbc3*, which were upregulated by *Trp53*, rescued *Rb1*-deficient cells from undergoing cell cycle arrest and apoptosis. These results suggest that the CDKN1B-RB1-E2F1 pathway is essential for SSC self-renewal and protects SSCs against genomic damage.
Key words: Apoptosis, Cell cycle arrest, Genomic damage, Rb1, Trp53

Spermatogenesis is a unique process that produces mature gametes and consists of three phases: amplification of spermatogonia, genetic diversification in spermatocytes and maturation of spermatids to spermatozoa to acquire mobility [1, 2]. Because parental genetic information must be preserved faithfully for the next generation, germ cells are thought to maintain a stable genetic integrity compared with somatic cells. Although little is known regarding the mechanism, germ cells may protect their pristine genome through different strategies. Of the different spermatogenic cell types, spermatogonial stem cells (SSCs) are the only cell type with self-renewal potential. These cells continuously undergo mitotic divisions and produce enormous amounts of committed progenitors during their lifetime. SSCs are thought to consist of ~5–10% of A_{single} (A_s) spermatogonia [3, 4]. Since SSCs are the founder population of spermatogenesis, the maintenance of SSC genetic integrity is of utmost importance. Furthermore, the accumulation of genetic abnormalities in SSCs can lead to the suppression of spermatogenesis and thus infertility.

Despite their apparent biological importance, SSC analysis has been challenging because of their low frequency in the testis and the lack of SSC-specific markers. However, SSC culture techniques have allowed us to study SSCs *in vitro* [5]. SSCs can be cultured for long periods of time in the presence of glial cell line-derived neurotrophic factor (GDNF) and fibroblast growth factor 2 (FGF2). Cultured SSCs, designated as germline stem (GS) cells, proliferate *in vitro* as grape-like clusters of spermatogonia on mouse embryonic fibroblasts (MEFs). These cells initiate spermatogenesis upon introduction into seminiferous tubules of infertile testes. One of the most important findings from culture studies was the stable genetic and epigenetic integrity of SSCs [6]. GS cells were shown to maintain a normal number of chromosomes and androgenetic imprinting patterns despite 2 years of consecutive cultures. This result was unexpected given that many cultured cells undergo senescence and exhibit karyotype abnormalities and abnormal DNA methylation. Although factors involved in the maintenance of genetic integrity have not been identified, these results confirmed that replication of genetic information in SSCs proceeds with higher fidelity.

Our understanding of the signaling pathway of self-renewal factors, however, has improved. GDNF is known to activate HRAS via *Src* family kinase molecules [7, 8], and cells transfected with activated *Hras* undergo self-renewal division without exogenous cytokines [7]. Activation of HRAS increases the expression of *Ccnd2* and *Ccne1*. Overexpression (OE) of both *Ccnd2* and *Ccne1* in GS cells allows cytokine-free self-renewal in a manner similar to *Hras*-transfected cells. Although these cells are known to have SSC activity based on a transplantation assay, both types of GS cells produced germ cell tumors in recipient mice, suggesting that excessive stimulation of self-renewal triggers tumor formation. *Hras* and *Ccnd2* play similar roles in humans, because human germ cell tumors show enhanced expression of *Hras* and *Ccnd2* [9, 10]. While these previous studies revealed the critical role of G1/S cyclins in self-renewal, how they regulate the G1/S transition in SSCs remains unknown. Cyclins bind to cyclin-dependent kinase (CDK) and phosphorylate RB1 [11]. RB1 phosphorylation causes changes in cell cycle-related genes, including E2F1 activation. Understanding the dynamics of these molecules is a prerequisite for clarifying the link between cytokine signaling and self-renewal.

Two recent studies have addressed the function of *Rb1* in SSCs. One study showed that *Rb1* deficiency caused progressive loss of GFRA1-positive (GFRA1$^+$) A$_s$ spermatogonia when the *Rb1* gene was deleted by *Cre* driven by the *Ddx4* promoter [12]. The *Ddx4* promoter became active during embryonic development at ~15.5 days post coitum (dpc). *Rb1*-deficient A$_s$ spermatogonia incorporated 5-bromo-2-deoxyuridine (BrdU) at a similar rate as controls and did not show increased apoptosis. Notably, A$_s$ spermatogonia generated no A$_s$ spermatogonia, only A$_{paired}$ (A$_{pr}$) spermatogonia upon *Rb1* loss. In contrast, another group suggested that SSCs do not form in *Ddx4-Cre Rb1*$^{flox/-}$ mice and reported that the loss of *Rb1* influenced SSC maturation from gonocytes [13]. When *Stra8-* or *Neurog3-Cre* transgenic mice that express *Cre* in undifferentiated spermatogonia were used to delete *Rb1*, these mice showed normal spermatogenesis, suggesting that *Rb1* may play a role in the transition of gonocytes to SSCs. Although SSC self-renewal was shown to be repressed in pup testis cells, this study involved small interfering RNA (siRNA)-mediated partial knockdown (KD), and this conclusion does not agree with the observation that germ cells, which were suggestive of SSCs, were present in mature *Ddx4-Cre Rb1*$^{flox/-}$ mice. Thus, although both studies showed the critical role of *Rb1* in male germline cells, they reached different conclusions regarding the role of *Rb1*. Moreover, they did not address how molecules involved in the G1/S transition regulate *Rb1*, and the precise function and the mechanism of action of *Rb1* in postnatal SSCs remain elusive.

In this study, we extended our previous observations and analyzed the molecular mechanism of the G1/S transition in GS cells. We found that depletion of the CDK inhibitor (CDKI) *Cdkn1b* decreased CDK4 and RB1 levels in GS cells. Moreover, we found that *Rb1* deficiency induced DNA double-strand breaks (DSBs) in GS cells and that *Rb1*-deficient GS cells were arrested at the G2/M phase and underwent apoptosis. This cell cycle suppression and apoptosis could be rescued by depletion of *Trp53*, which protects the genome. Thus, the network involving *Trp53* and *Rb1* governs the genetic integrity and maintenance of SSCs.

Materials and Methods

Animals and transplantation

Rb1$^{flox/flox}$ mice were obtained from the NCI Mouse Models of Human Cancers Consortium (NCI Mouse Repository, Frederick, MD, USA) [14]. These mice were crossed with *R26R* female mice to introduce the *LacZ* reporter construct for *Cre*-mediated deletion [15] (The Jackson Laboratory, Bar Harbor, ME, USA). For production of *Ddx4-Cre Rb1*$^{flox/-}$ mice, *Rb1*$^{flox/flox}$ mice were mated with *Ddx4-Cre* transgenic mice (The Jackson Laboratory). The genotypes of the mice were examined by polymerase chain reaction (PCR) with the primers listed in Supplementary Table 1 (online only). For deletion of *Rb1 in vitro*, dissociated testis cells were exposed to adenovirus expressing *Cre* (AxCANCre, RIKEN BRC, Tsukuba, Japan) at a density of 1 × 10^6 cells/9.5 cm^2, as described previously [16]. After an overnight incubation, the virus was removed on the next day, and cells were used for transplantation. The multiplicities of infection (MOIs) were adjusted to 2.0. For transplantation, testis cells were dissociated into a single-cell suspension using a two-step enzymatic digestion with collagenase type IV and trypsin (Sigma, St Louis,

MO, USA), as described previously [17]. Cells were transplanted into seminiferous tubules of WBB6F1-W/W^v (designated W) mice (Japan SLC, Hamamatsu, Japan) through the efferent duct [17]. For allogeneic transplantation, recipient mice were treated with anti-CD4 antibody, as described previously [18]. Approximately 4 µl could be introduced into each testis, which filled 75–85% of the seminiferous tubules. The Institutional Animal Care and Use Committee of Kyoto University approved all animal experimentation protocols.

Cell culture

GS cells were established from B6/Tg14 (act-EGFP-OsbY01) mice (a gift from Dr M Okabe, Osaka University, Japan) or B6-TgR (ROSA26)26Sor (ROSA; The Jackson Laboratory) mice that were backcrossed to a DBA/2 background for at least 7 generations [5, 19]. GS cells from *Trp53* KO mice were previously described [20]. We also derived *Rb1*$^{flox/flox}$ GS cells from 4- to 5-day-old *Rb1*$^{flox/flox}$ mice, which were produced by mating F$_1$ offspring that resulted from crossing of *Rb1*$^{flox/+}$ mice in a B6 background to ICR mice. AxCANCre was added to these cells at MOIs of 2.0 to produce *Rb1* KO GS cells. AxCANLacZ (RIKEN BRC) was used as a control. The conditions of GS cell culture using StemPro-34 SFM (Invitrogen, Carlsbad, CA, USA) were described previously [5]. The growth factors used were 10 ng/ml human FGF2 and 15 ng/ml rat GDNF (Peprotech, Rocky Hill, NJ, USA). The cells were maintained on mitomycin C (Sigma)-treated MEFs.

Gene expression analyses

Total RNA was recovered using TRIzol reagent (Invitrogen), and first-strand cDNA was produced using a Verso cDNA Synthesis Kit (Thermo Fisher Scientific, Waltham, MA, USA) for reverse transcription (RT)-PCR. For real-time PCR, a StepOnePlus^{TM} Real-Time PCR System (Applied Biosystems, Warrington, UK) and FastStart Universal SYBR Green Master Mix (Roche Applied Science, Mannheim, Germany) were used according to the manufacturers' protocols. Transcript levels were normalized relative to those of *Hprt*. The real-time PCR conditions were 95 C for 10 min, 40 cycles at 95 C for 15 sec, and then 60 C for 1 min. Each PCR was performed at least in triplicate, and gene expression levels were determined with at least three biological repeats. For RT-PCR, the PCR conditions were 95 C for 5 min followed by 30 cycles at 94 C for 30 sec, 60 C for 30 sec and 72 C for 30 sec. The primers used for PCR are listed in Supplementary Table 1.

Lentivirus infection

For gene OE experiments, PSM-human *Rb1* (Addgene, Cambridge, MA, USA), human papillomavirus E7 (Addgene), mouse *Bbc3* (transOMIC technologies, Huntsville, AL, USA), mouse *Cdkn1a* (Addgene) and mouse *Cdkn2a* (*p16*; Addgene) were cloned into the CSII-EF-IRES2-Venus vector. For *E2f1* OE, mouse *E2f1* cDNA containing the full-length open reading frame was amplified by PCR and cloned into the CSII-EF-IRES2-Venus vector. Lentivirus particles were produced by transient transfection of 293T cells, and GS cells or testes cells were transfected as described previously [21]. CSII-EF-MCS-IRES2-Venus was used as a control. Titers of the virus were determined by transfecting 293T cells, and the MOIs were adjusted to 4.0. For gene KD experiments, KD vectors

for *Cdk4*, *Cdk6*, *Cdkn1b*, *E2f1* and *Bbc3* were obtained from Open Biosystems (Huntsville, AL, USA). For *Trp53* KD, we used pSicoR *Trp53* and its control vector pSicoR (Addgene). For *Cdkn1a* KD, we used pFUGWH1-*Cdkn1a* and its control vector pFUGWH1 (a gift from Dr S Temple, Neural Stem Cell Institute, Rensselaer, NY, USA). A mixture of lentivirus particles was used to transfect GS cells from *Rb1*flox/flox or ROSA mice. pLKO1-Scramble shRNA was used as a control (Addgene). The lentivirus titer was determined using a Lenti-X p24 Rapid Titer Kit (Clontech, Mountain View, CA, USA). KD vectors from Open Biosystems are listed in Supplementary Table 2 (online only).

Analyses of recipient testes

Recipient mice were killed at the indicated time points, and their testes were analyzed by staining for β-galactosidase with 5-bromo-4-chloro-3-indolyl-β-D-galactopyranoside (X-gal; Wako Pure Chemical Industries, Osaka, Japan) [19]. A germ cell cluster was defined as a colony when it occupied the entire basal surface of the tubule and was longer than 0.1 mm. For histological analysis, paraffin-embedded sections were stained with hematoxylin and eosin. The number of tubules with spermatogenesis, as defined by the presence of multiple layers of germ cells in the entire circumference of the tubules, was recorded for one section from each testis.

Western blotting

Samples were separated by SDS-PAGE and transferred onto Hybond-P membranes (GE Healthcare, Piscataway, NJ, USA). The membranes were incubated with primary antibodies. The antibodies used in the experiments are shown in Supplementary Table 3 (online only).

Southern blotting

Genomic DNA was digested with *Pst*I and transferred and hybridized with the exon 18 probe [22], as described previously [16]. The PCR product was subsequently cloned into the pGEMT easy vector (Promega, Madison, WI, USA). The plasmid was then digested with *Eco*RI to produce a 492-bp fragment, which was used as a hybridization probe. Band intensity was quantified using the ImageJ 1.43r software (US National Institutes of Health, Bethesda, MD, USA).

Flow cytometry

For analysis of cell surface markers, GS cells were stained in phosphate-buffered saline (PBS)/1% fetal bovine serum (FBS) using the antibodies listed in Supplementary Table 3. For cell cycle analysis, GS cells were incubated with Hoechst 33342 (12.5 μg/ml; Sigma) for 30 min at 37 C and suspended in PBS/1% FBS. For quantification of cell cycle phases using combined propidium iodide (PI) and BrdU staining, GS cells were cultured in the presence of BrdU (50 μM; BD Biosciences, San Jose, CA, USA) for 6 h. After fixation by ethanol, cells were treated with HCl (2N) for 20 min at room temperature. The cells were then incubated with Alexa 647-conjugated anti-BrdU antibody for 30 min and treated with 5 μg/ml PI and 100 μg/ml RNaseA for 30 min before analysis. Stained cells were analyzed using a FACSCalibur (BD Biosciences).

Apoptosis assay

To perform a terminal deoxynucleotidyl transferase biotin-dUTP nick-end labeling (TUNEL) assay, a single cell suspension was concentrated on glass slides by centrifugation with Cytospin 4 (Thermo Electron, Altrincham, UK). After fixation in 4% paraformaldehyde for 1 h, cells were labeled using an In Situ Cell Death Detection Kit, TMR red (Roche Applied Science), according to the manufacturer's protocol. The nuclei were counterstained with Hoechst 33342 (2 μg/ml; Sigma) to determine the percentage of TUNEL-positive nuclei relative to the total number of Hoechst 33342-stained nuclei. Apoptotic cells were quantified by collecting images of stained cells using the Photoshop software (Adobe Systems, San Jose, CA, USA).

Karyotype analysis

Cells were incubated with colcemid solution (60 ng/ml; KaryoMAX; Invitrogen) for 1 h, recovered by trypsin and treated with 75 mM KCl for 7 min. Metaphase spreads were prepared using a standard procedure after fixing the cells with methanol/acetic acid (3:1). The slides were stained with Hoechst 33342 (Sigma).

Comet assay

A comet assay was performed using a CometAssay Kit (Trevigen, Gaithersburg, MD, USA) according to the manufacturer's protocol. Briefly, GS cells were cultured for 2 weeks after adenovirus infection and suspended in PBS (2×10^5 cells/ml). The cell suspension was mixed with CometAaay LM Agarose (Trevigen) at a ratio of 1:10, and 50 μl was transferred to a CometSlide (Trevigen) for immobilization. After incubation in lysis solution, cells were treated with an alkaline solution for 30 min followed by electrophoresis. DNA was stained with SYBR Green I (TaKaRa Bio, Otsu, Japan). DNA damage was quantified by measuring the length of the visible comet tail. Cells with a ratio greater than or equal to 2 were counted as positive for DNA damage. Figures show the percentage of cells positive for DNA damage per treatment.

Immunostaining

Testes samples were fixed in 4% paraformaldehyde for 2 h and then frozen in Tissue-Tek O.C.T. Compound (Sakura Finetechnical, Tokyo, Japan). For immunostaining, samples were treated with 0.1% Triton-X in PBS. After immersion in blocking buffer (0.1% Tween 20, 3% bovine serum albumin and 10% goat or donkey serum in PBS), samples were incubated with primary antibodies at 4 C overnight. Secondary antibodies were incubated for 1 h at room temperature. Samples were counterstained with Hoechst 33342 (Sigma). Images were collected using a confocal microscope (Fluoview FV1000D; Olympus, Tokyo, Japan). The antibodies used are listed in Supplementary Table 3.

Statistical analyses

The results are presented as means ± SEM. Significant differences between means for single comparisons were determined using the Student's *t*-test. Multiple comparison analyses were performed using analysis of variance followed by Tukey's honestly significant differences test.

Results

Depletion of Cdk4 impairs GS cell proliferation

To examine the mechanism of the G1/S transition in GS cells, we first analyzed the role of *Cdk4* and *Cdk6*, which are regulated by G1/S cyclins to drive the cell cycle. We transduced GS cells with lentiviruses expressing short hairpin RNA (shRNA) against *Cdk4* or *Cdk6*. GS cells that had been depleted of either *Cdk4* or *Cdk6* proliferated more slowly compared to non-depleted controls (Fig. 1A; Supplementary Fig. 1A, online only). Since the SSC frequency in GS cell cultures is low (1–2%) [5], we confirmed the effect of gene depletion on SSCs based on germ cell transplantation into the seminiferous tubules of congenitally infertile W mice that lack endogenous spermatogenesis [23]. Analysis of the recipient testes showed that depletion of *Cdk4*, but not *Cdk6*, decreases SSC activity (Figs. 1B and C). The numbers of colonies generated by GS cells expressing shRNA against *Cdk4*, *Cdk6* and the control luciferase gene were 6.3 ± 6.3, 25.0 ± 13.4 and 50.0 ± 13.4 per 10^5 cells (n = 8), respectively, suggesting that *Cdk4* is responsible for the G1/S transition in SSCs.

We next examined the involvement of *Rb1* family genes, the major target of the CDK4-CCND complex. RB1 was phosphorylated upon addition of GDNF and FGF2 (Fig. 1D), which promote GS cell proliferation. When we analyzed RB1 expression levels using Western blotting, *Cdk4* depletion significantly decreased both the phosphorylated form and the total amount of RB1 (Fig. 1E).

We then examined the impact of *Cdkn1b* depletion on RB1 phosphorylation because CDKN1B is involved in stabilizing the CDK4/6-CCND complex in somatic cells [11]. In spermatogonia, we previously found (using serial transplantation) that SSC self-renewal is decreased in *Cdkn1b* knockout (KO) SSCs [24]. Consistently, *Cdkn1b* depletion inhibited GS cell proliferation and reduced the levels of RB1 and CDK4 in GS cells (Figs. 1F and G). These results suggested that *Cdk4* and *Cdkn1b* play critical roles in regulating RB1 function in GS cells.

Rb1 deficiency impairs SSC activity

To examine the function of *Rb1* in SSCs, we first used phosphorylation site-mutated RB1 (PSM-RB1), a constitutive active mutant of RB1 [25]. PSM-RB1 has been shown to cause G1 arrest and to interfere with S phase progression. We transfected GS cells with a lentivirus expressing PSM-RB1 and found that PSM-RB1 significantly reduced the GS cell number (Fig. 2A), suggesting that excessive activation of RB1 abrogates self-renewal of SSCs. To examine whether diminished RB1 influences self-renewal, we next used human papillomavirus E7 oncoprotein, which induces degradation of RB1 through the ubiquitin-proteasome pathway [26]. *E7* OE significantly lowered GS cell proliferation compared with the control (Fig. 2B). These results suggested that appropriate activity levels of RB1 are important for driving self-renewal division.

Based on these results, we used *Rb1* floxed mice to confirm the role of *Rb1* function on freshly isolated SSCs [14]. These mice were mated with *R26R* reporter mice to visualize the colonization of donor cells [15]. Testis cells were collected from 9-day-old pup testes and dissociated into single cells. Littermates were used as controls. The cells were then exposed to an AxCANCre overnight *in vitro*
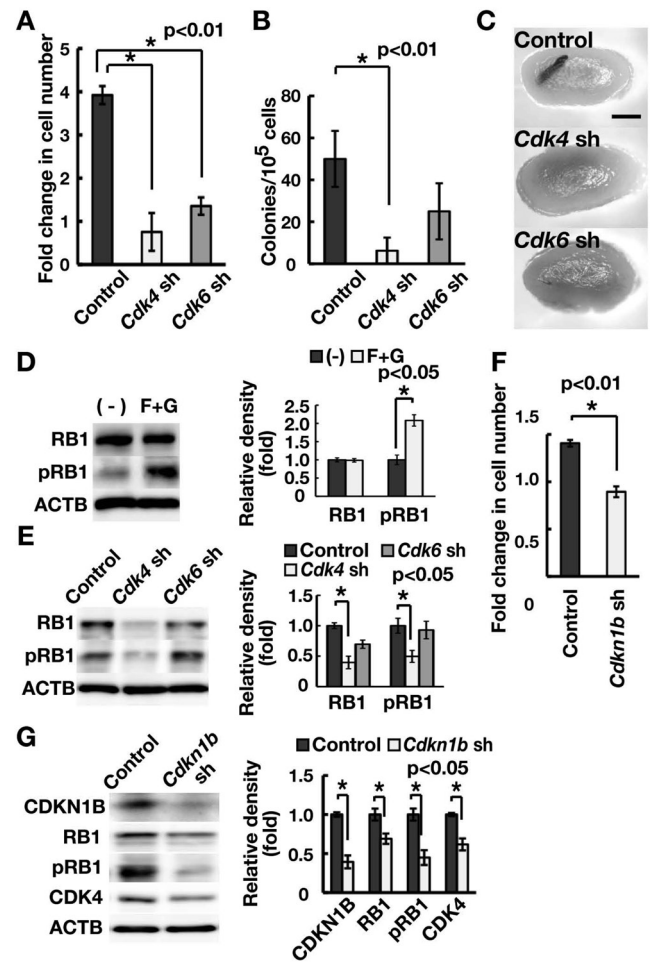

Fig. 1. Regulation of RB1 in spermatogonia. (A) Suppression of GS cell proliferation through depletion of *Cdk4* or *Cdk6*. GS cells were infected with the indicated lentivirus expressing shRNA and passaged 4 days after transfection. Cell recovery was determined 6 days after passage (n = 4; MOI = 10). (B) Colony counts. Cells were transplanted 2 days after transfection. Results of two experiments (n = 8; MOI = 10). (C) Macroscopic appearance of recipient testes that received transplantation of GS cells depleted of *Cdk4* or *Cdk6*. (D) Western blot analysis of RB1. GS cells were cultured without cytokines for 3 days and stimulated with FGF2 and GDNF. Cells were recovered 1 h after cytokine stimulation. Note the relative increase in phosphorylated RB1 (pRB1) caused by cytokine stimulation. The graph shows relative band intensity (n = 3). (E) Western blot analysis of RB1 following depletion of *Cdk4* or *Cdk6*. Cells were recovered 4 days after transfection (MOI = 10). The graph shows relative band intensity (n = 3). (F) Suppression of GS cell proliferation through depletion of *Cdkn1b*. GS cells were infected with the indicated lentivirus, and cells were recovered 4 days after transfection (n = 4; MOI = 4). (G) Western blot analysis of cell cycle-related proteins following depletion of *Cdkn1b*. Cells were recovered 4 days after transfection (MOI = 4). The graph shows relative band intensity (n = 3). Bar = 1 mm (C).

[16]. Southern blot analysis of the *Cre*-infected cells revealed that the deletion efficiency of *Rb1* was 49.1–54.7% (with an average of 52.6%) at the time of cell recovery (Fig. 2C). The recovered cells were transplanted into W mice. Three separate experiments were
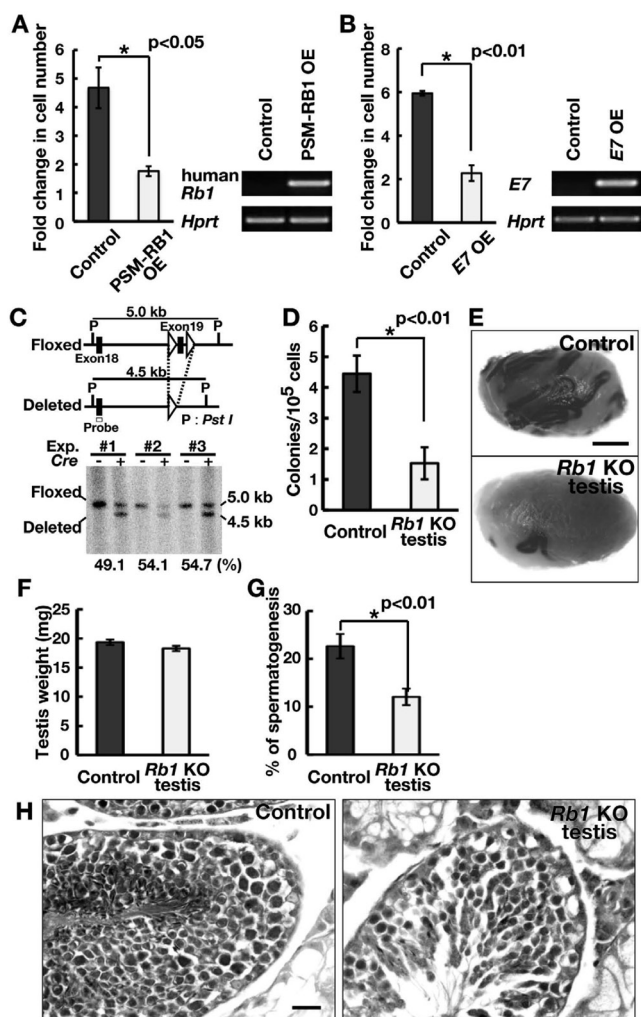
Fig. 2. Functional analysis of *Rb1* in self-renewal division. (A) Suppression of GS cell proliferation following transfection of constitutively active RB1 (PSM-RB1). GS cells were infected with the indicated lentivirus and passaged 4 days after transfection. Cell recovery was determined 6 days after passage (n = 3; MOI = 10). OE was confirmed by RT-PCR 2 days after transfection. (B) Suppression of GS cell proliferation following transfection of *E7*. GS cells were infected with the indicated lentivirus and passaged 4 days after transfection. Cell recovery was determined 6 days after passage (n = 3; MOI = 10). OE was confirmed by RT-PCR 2 days after transfection. (C) Conditional mutant mice used in the experiment. Exon 19 of the *Rb1* gene was deleted using *Cre*-mediated recombination. The indicated probe was used for Southern blot analysis. (D) Colony counts. Results of three experiments (n = 12). (E) Macroscopic appearance of recipient testis. (F) Testicular weight (n = 8). (G) Tubules with spermatogenesis, defined as the presence of multiple layers of germ cells in the entire circumference of the tubules. At least 169 tubules were counted (n = 7). (H) Histological appearance of recipient testis. Bar = 1 mm (E), 20 μm (H).

performed involving 12 testes for each cell type.

Analysis of the recipient testes showed that the numbers of colonies produced by *Rb1* KO and control testis cells were 1.5 ± 0.5 and 4.4 ± 0.6 (n = 12) per 10^5 cells, respectively (Fig. 2D and

E), and the difference was significant. Although the weights of the recipient testes were comparable (Fig. 2F), histological analysis of the recipient testes revealed that the number of tubules with spermatogenesis significantly decreased in testes transplanted with *Rb1* KO testis cells (Fig. 2G and H). These results suggest that *Rb1* is required for SSC activity.

Rb1 deficiency increases apoptosis and cell cycle progression

To characterize the mechanism of *Rb1* function in SSC activity, we derived GS cells from *Rb1flox/flox* mice and examined their response upon *Cre*-mediated *Rb1* deletion (Fig. 3A). Although we observed no apparent changes in colony morphology upon *Cre*-mediated gene deletion, we noted that CRE exposure significantly reduced cell recovery (Fig. 3B). Due to the close association of *Rb1* with cell cycle progression, we performed flow cytometry to examine the impact of *Rb1* deficiency on cell cycle progression (Fig. 3C). Analysis using Hoechst 33342 showed that *Rb1* deficiency increases the number of GS cells at the G2/M phase of the cell cycle, and this is accompanied by a relative decrease in the G1 phase. Further analysis using BrdU staining confirmed these results (Fig. 3D). Since we observed an increase in the sub-G0 population by flow cytometry (Fig. 3D), we performed TUNEL staining to directly examine apoptosis levels (Fig. 3E). Our results showed that the frequency of TUNEL-positive (TUNEL+) cells increased significantly upon *Rb1* deletion compared with the control.

Because loss of SSC activity can occur due to increased differentiating divisions, we also examined the expression of several spermatogonia markers. Real-time PCR analysis showed that *Rb1* deficiency significantly decreased the expression of *Gfra1* and *Ret*, both of which comprise a GDNF receptor (Fig. 3F) [27]. However, we observed no apparent changes in cell surface marker expression using flow cytometry (Fig. 3G). We also detected increased expression of differentiation markers at the mRNA level. However, only *Sox3* was expressed more strongly in *Rb1* KO GS cells, and the remaining differentiation markers were not affected by *Rb1* deficiency.

E2f1 OE decreases SSC activity

To characterize the molecules underlying the phenotype of *Rb1* KO GS cells, we first analyzed the role of *E2f1*. E2F1 is released from RB1 when RB1 is phosphorylated by the CDK-cyclin complex in somatic cells [28]. In spermatogonia, previous studies using transgenic mice showed that *E2f1* OE *in vivo* induces apoptosis of spermatogonia and severe testicular atrophy [29]. *E2f1* KO mice also showed a gradual loss of spermatogenesis, which is thought to be caused by depletion of SSCs [30, 31].

To examine the role of *E2f1* in SSCs, we used GS cells. Transfection experiments showed that *E2f1* OE reduced the number of GS cells (Fig. 4A; Supplementary Fig. 1B, online only). To directly examine whether *E2f1* OE has any impact on SSCs, we transplanted *E2f1*-transfected GS cells into the seminiferous tubules of W mice. Analysis of the recipient mice showed that the numbers of colonies generated by *E2f1* OE and control GS cells were 31.3 ± 13.2 and 100. 0 ± 21.1 per 10^5 cells (n = 8), respectively (Figs. 4B and C). These results indicate that excessive *E2f1* activity reduces the SSC concentration in GS cell cultures.

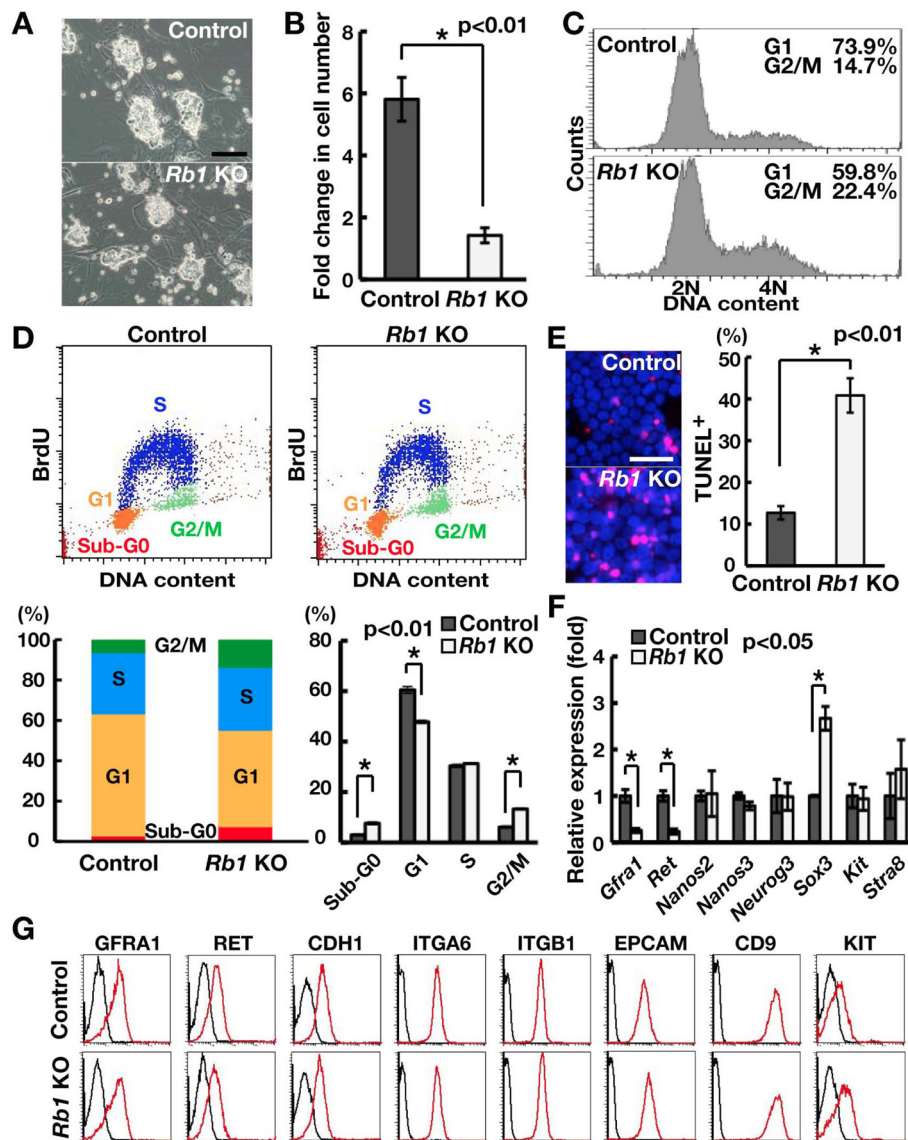To understand the function of E2F1, we examined the apoptosis

Fig. 3.   Increased apoptosis and abnormal cell cycle progression of *Rb1* KO GS cells. (A) Appearance of *Rb1* KO GS cells. (B) Impaired proliferation of *Rb1* KO GS cells (n = 3). Cells were recovered 2 weeks after AxCANCre transfection. (C) Analysis of cell cycle distribution using Hoechst 33342. Cells were analyzed 2 weeks after AxCANCre transfection. (D) Quantification of cell cycle phases by combined propidium iodide and BrdU staining. Cells were analyzed 2 weeks after AxCANCre transfection (n = 3). (E) Quantification of apoptotic cells using TUNEL staining (n = 3). At least 273 cells were counted 1 week after AxCANCre transfection. (F) Real-time PCR analysis of spermatogonia markers (n = 6). (G) Flow cytometric analysis of cell surface markers. Bar = 50 μm (A, E).

level of *E2f1*-transfected GS cells. TUNEL staining showed that *E2f1* OE increases apoptosis of GS cells within 10 days (Fig. 4D). E2F1 is known to cause apoptosis through several pathways [32] and is considered a strong regulator of apoptosis after DNA damage in many cancers [32]. Therefore, although *Rb1* KO GS cells contained a normal chromosome number (Fig. 4E), *Rb1* deficiency may induce DNA DSBs by activating E2F1. To test this hypothesis, we performed immunocytochemistry of *Rb1* KO GS cells. Analysis of *Rb1* KO GS cells showed enhanced staining of DNA DSB markers, including γH2AX, RAD51 and TRP53BP1 (Figs. 4F–H; Supplementary Figs.

2A–C, online only). To further confirm whether the increase in γH2AX staining corresponded to DNA damage, we subjected *Rb1* KO GS cells to a comet assay, which revealed increases in tail DNA content in *Rb1* KO GS cells (Fig. 4I).

Increased γH2AX staining was also observed in *E2f1*-transfected GS cells (Fig. 4J). Because E2F1 is activated by *Rb1* deficiency, we depleted *E2f1* in *Rb1* KO GS cells to examine whether *E2f1* is required for DNA DSBs. Immunocytochemical staining showed that depletion of *E2f1* could suppress increases in γH2AX staining in *Rb1* KO GS cells (Fig. 4K; Supplementary Fig. 1A). These results
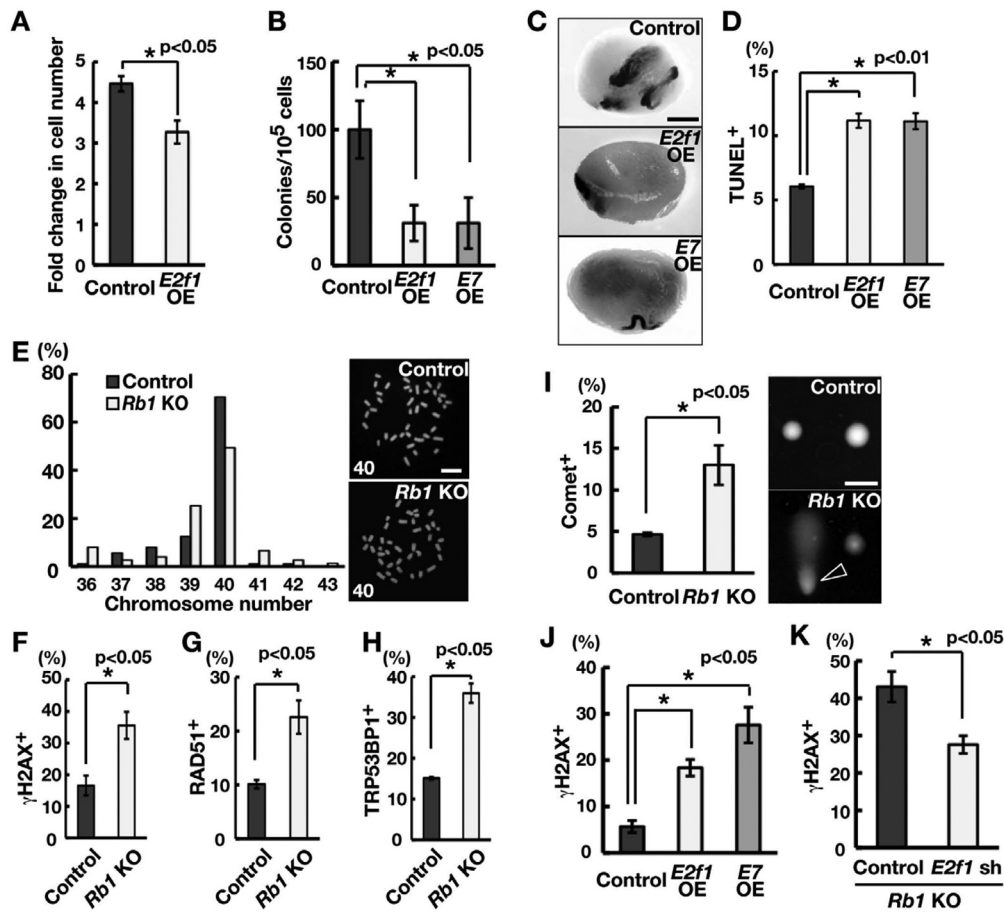
Fig. 4. Induction of DNA DSBs by E2F1 activation. (A) Suppression of GS cell proliferation following transfection of *E2f1*. GS cells were infected with the indicated lentivirus and passaged 4 days after transfection. Cell recovery was determined 6 days after passage (n = 3; MOI = 10). (B) Colony counts. Results of two experiments (n = 8). (C) Macroscopic appearance of recipient testis. (D) Quantification of apoptotic cells following *E2f1* or *E7* OE using TUNEL staining. At least 536 cells were counted 10 days after AxCANCre transfection. Results of four experiments (MOI = 10). (E) Karyotype analysis and metaphase spread of GS cells. Cells were analyzed 2 weeks after AxCANCre transfection (n = 88 for control; n = 75 for KO). The number in the metaphase spread indicates the chromosome number. (F–H) Quantification of γH2AX- (F), RAD51- (G) and TRP53BP1 (H)-positive cells of *Rb1* KO GS cells. Cells were recovered 2 weeks after AxCANCre transfection (n =3). At least 338 (F), 401 (G) and 149 (H) cells were counted. Representative pictures are shown in Supplementary Fig. 2 (online only). (I) Comet assay. Data are expressed as the percent damage compared with the control sample. The arrowhead indicates a cell with DNA damage. (J) Immunocytochemistry of GS cells transfected with *E2f1* or *E7* for γH2AX. Cells were recovered 10 days after transfection (n = 3). At least 304 cells were counted. (K) Suppression of γH2AX staining following depletion of *E2f1*. Cells were co-transfected with AxCANCre and a lentivirus expressing shRNA against *E2f1* and recovered 6 days after transfection (n = 3; MOI = 4). At least 252 cells were counted. Bar = 1 mm (C), 50 μm (E, I).

suggested that activation of E2F1 by *Rb1* deficiency causes DNA DSBs and apoptosis, thereby reducing SSC activity.

Rb1 deficiency activates Trp53 and increases pro-apoptotic gene expression

We next examined how *Rb1* deficiency causes apoptosis and cell cycle arrest. We hypothesized that DNA damage induced by *E2f1* OE activates TRP53. We first performed Western blot to examine TRP53 levels (Fig. 5A). Although *Rb1* deficiency did not change the amount of total TRP53, it induced phosphorylation at Ser23 and Ser46, both of which have been implicated in the DNA damage response [33, 34]. Consistent with our hypothesis, depletion of *Trp53* rescued the reduced recovery of GS cells upon *Rb1* deletion (Fig. 5B). Because

this result suggested activation of the TRP53-mediated apoptosis pathway, we examined the impact of *Trp53* depletion on *Rb1* KO GS cells and found that depletion of *Trp53* by shRNA significantly suppressed apoptosis of *Rb1* KO GS cells (Fig. 5C). Although combined deficiency of *Trp53* and *Rb1* can cause transformation of somatic cells [35], we found no clear evidence of transformed GS cells after depletion of *Trp53*. However, when we transfected *Trp53* KO GS cells with *E7*, cells proliferated more actively (Fig. 5D), suggesting that *Rb1* suppresses the proliferation of *Trp53* KO GS cells.

To examine the mechanism of *Trp53*-induced apoptosis, we examined the expression of apoptosis-related genes that are regulated by *Trp53*. Our screening using real-time PCR revealed that *Rb1* KO
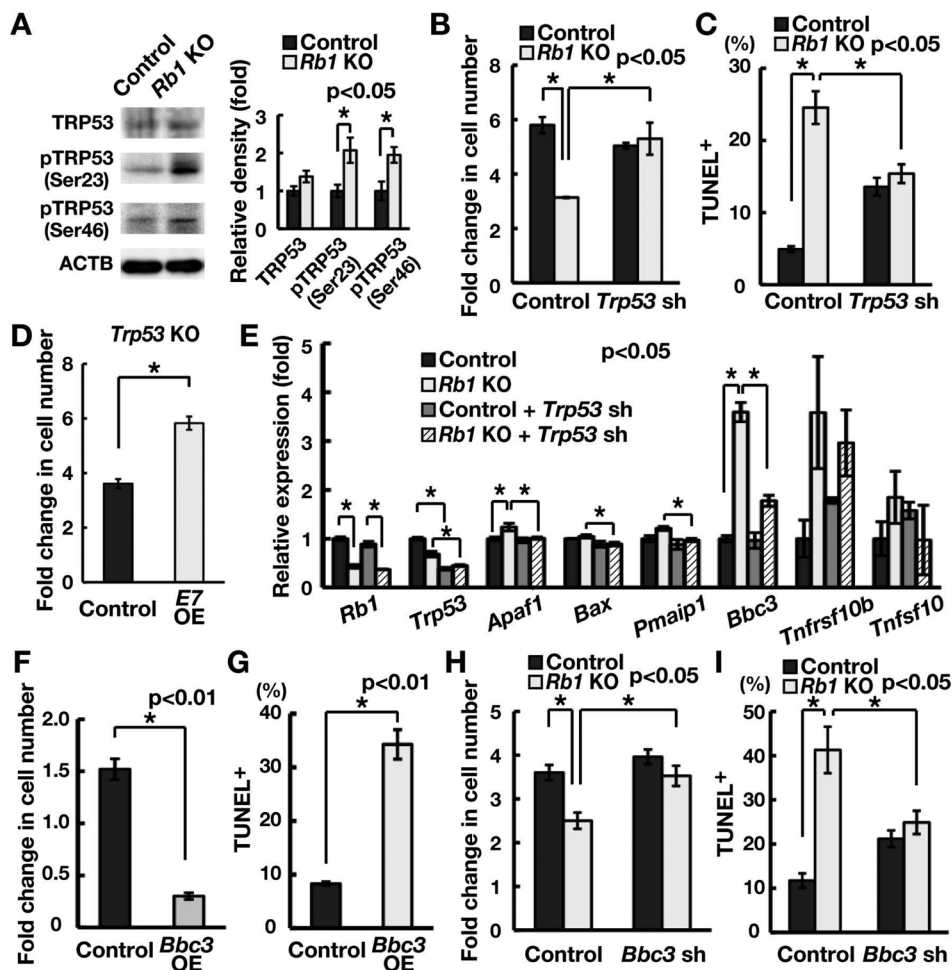
Fig. 5. Increased *Bbc3* expression causes apoptosis of GS cells upon *Rb1* deletion. (A) Western blot analysis of TRP53. Cells were recovered 3 days after AxCANCre transfection. The graph shows relative band intensity (n = 3). Note the relative increase in phosphorylated TRP53 (pTRP53) in *Rb1* KO GS cells. (B) Increased recovery of *Rb1* KO GS cells following depletion of *Trp53*. Cells were transfected with AxCANCre and a lentivirus expressing shRNA against *Trp53* and recovered 1 week after infection (n = 3; MOI = 4). (C) Quantification of apoptotic cells using TUNEL staining following depletion of *Trp53* (n = 3). Cells were transfected with AxCANCre and a lentivirus expressing shRNA against *Trp53* (MOI = 4) and recovered 1 week after infection. At least 545 cells were counted in three experiments. (D) Increased cell recovery of *E7*-transfected *Trp53* KO GS cells (n = 3; MOI = 10). Cells were transfected with a lentivirus expressing *E7* and passaged 4 days after transfection. Cells were recovered 6 days after passage. (E) Real-time PCR analysis of apoptosis-related genes following *Rb1* gene deletion. Cells were transfected with AxCANCre and a lentivirus expressing shRNA against *Trp53*, and recovered 3 days after infection (n = 3; MOI = 4). (F) Reduced GS cell recovery upon *Bbc3* OE. GS cells were transfected with a lentivirus expressing *Bbc3*. Cells were recovered 4 days after transfection (n = 3; MOI = 10). (G) Quantification of apoptotic cells after *Bbc3* OE using TUNEL staining (n = 3; MOI = 10). At least 239 cells were counted 4 days after transfection. (H) Increased recovery of *Rb1* KO GS cells following depletion of *Bbc3*. Cells were transfected with AxCANCre and a lentivirus expressing shRNA against *Bbc3* and recovered 1 week after infection (n = 6; MOI = 10). (I) Quantification of apoptosis of *Rb1* KO cells using TUNEL staining after *Bbc3* depletion. Cells were transfected with AxCANCre and a lentivirus expressing shRNA against *Bbc3* and recovered 1 week after infection (n = 3; MOI = 10). At least 270 cells were counted.

GS cells showed increased expression of *Bbc3* (Fig. 5E). Although the level of *Tnfrsf10b* increased slightly, the increase was not significant. The increase in *Bbc3* was inhibited by *Trp53* depletion (Fig. 5E), confirming that it was activated by *Trp53*. To examine the function of *Bbc3*, we transfected *Bbc3* into GS cells. *Bbc3* OE decreased cell recovery and increased the number of cells undergoing apoptosis (Fig. 5F and G; Supplementary Fig. 1B). In contrast, *Bbc3* depletion increased the cell recovery of *Rb1* KO GS cells and reduced apoptosis levels (Fig. 5H and I; Supplementary Fig. 1A). These results suggested

that upregulation of *Bbc3* is responsible for the increased apoptosis caused by *Rb1* deficiency.

Induction of Cdkn1a blocks cell cycle progression following induction of Rb1 deficiency

We next examined cell cycle arrest in *Rb1* KO GS cells. When the expression of several cell cycle-related genes was examined using real-time PCR, no apparent changes were observed in cyclin expression (Fig. 6A). However, *Rb1* KO GS cells showed increased
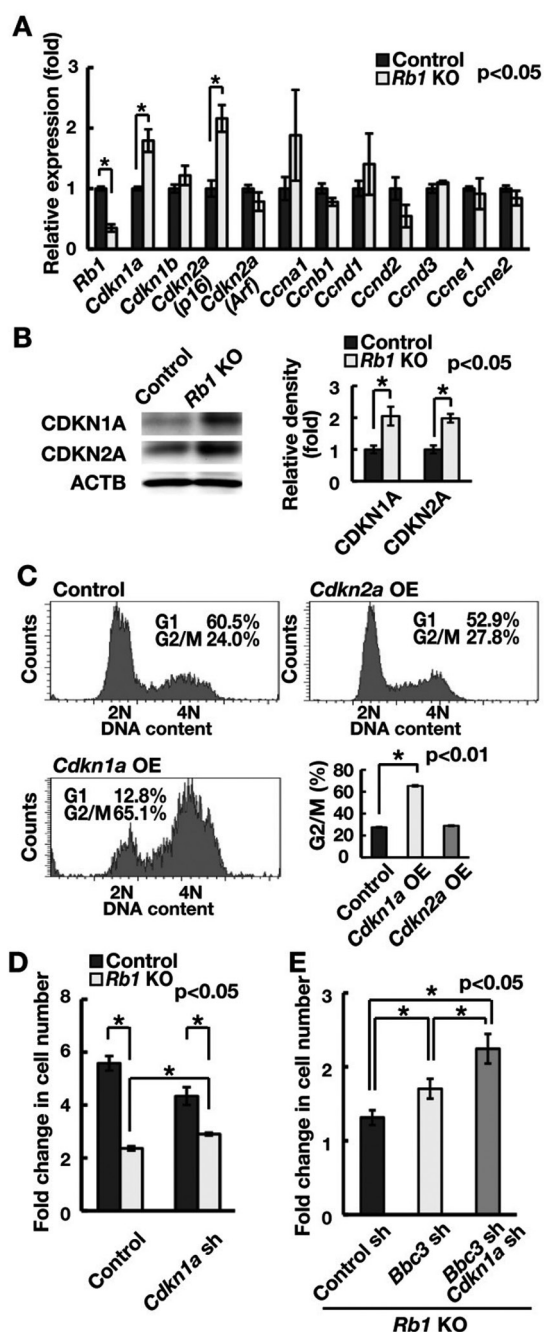
Fig. 6. Suppression of the cell cycle by *Cdkn1a* induction following induction of *Rb1* deficiency. (A) Real-time PCR analysis of cell cycle-related genes following *Rb1* gene deletion. Cells were recovered 2 weeks after AxCANCre transfection (n = 3). (B) Western blot analysis of CDKI proteins following *Rb1* gene deletion. Cells were recovered 2 weeks after AxCANCre transfection. The graph shows relative band intensity (n = 3). (C) Cell cycle analysis by Hoechst 33342 following *Cdkn1a* or *Cdkn2a* OE (MOI = 10). (D) Increased cell recovery of *Rb1* KO GS cells following depletion of *Cdkn1a*. Cells were transfected with AxCANCre and a lentivirus expressing shRNA against *Cdkn1a* and recovered 1 week after infection (n = 3; MOI = 4). (E) Increased cell recovery of *Rb1* KO GS cells following double depletion of *Bbc3* and *Cdkn1a*. Cells were transfected with AxCANCre and a lentivirus expressing shRNA against the indicated genes and recovered 1 week after infection (n = 8; MOI = 4).

expression of CDKIs *Cdkn1a* and *Cdkn2a* (*p16*), suggesting that upregulation of *Cdkn1a* and *Cdkn2a* (*p16*) caused cell cycle arrest. No increase in the levels of *Cdkn2a* (*Arf*), an important mediator of TRP53-dependent apoptosis induced by E2F1, was observed. Western blot analysis confirmed the increased expression of CDKN1A and CDKN2A (Fig. 6B). To explore whether *Cdkn1a* or *Cdkn2a* blocks the cell cycle of GS cells, GS cells were transfected with a lentivirus vector expressing either *Cdkn1a* or *Cdkn2a*. When *Cdkn1a* was transfected into GS cells, a significant number of cells were arrested at the G2/M phase (Fig. 6C; Supplementary Fig. 1B). Although *Cdkn2a* depletion similarly induced cell cycle arrest, its effect was not significant.

Because *Cdkn1a* is a *Trp53* downstream gene, this result suggested that activation of the *Trp53-Cdkn1a* pathway blocks cell cycle progression in *Rb1* KO GS cells. We examined this hypothesis by depleting *Cdkn1a* in *Rb1* KO GS cells. Analysis of the cell count after transfection showed that depletion of *Cdkn1a* increased the cell recovery after induction of *Rb1* deficiency (Fig. 6D; Supplementary Fig. 1A). Furthermore, double depletion of *Bbc3* and *Cdkn1a* synergistically improved cell recovery upon induction of *Rb1* deficiency (Fig. 6E). These results suggested that induction of *Trp53* activation reduced cell recovery upon induction of *Rb1* deficiency by upregulating *Bbc3* and *Cdkn1a* levels.

Increased DNA damage in undifferentiated spermatogonia of Ddx4-Cre Rb1^{flox/−} mice

In the final set of experiments, we analyzed undifferentiated spermatogonia in 10-day-old *Ddx4-Cre Rb1*^{flox/−} mice to examine the mechanism by which spermatogonia undergo depletion after prenatal loss of *Rb1*. We performed double immunohistochemistry using GFRA1, CDH1 and KIT. GFRA1 is highly expressed in A$_s$ and A$_{pr}$ spermatogonia and gradually decreases in A$_{aligned}$(A$_{al}$) spermatogonia [36]. CDH1 is expressed in the total undifferentiated spermatogonia population [37], while KIT is expressed in differentiating spermatogonia.

The number of GFRA1$^+$ cells was significantly decreased in *Ddx4-Cre Rb1*^{flox/−} mice, as reported in a recent study [12], and this was accompanied by increased expression of γH2AX, RAD51 and pTRP53 (Fig. 7A; Supplementary Fig. 3A, online only). In contrast, CDH1-positive (CDH1$^+$) cells were significantly increased in *Ddx4-Cre Rb1*^{flox/−} mice, as reported previously [12], despite the increased amount of DNA DSB markers and pTRP53 (Fig. 7B; Supplementary Fig. 3B, online only). The number of KIT-expressing cells showed no significant changes, but γH2AX-positive (γH2AX$^+$) cells significantly increased (Fig. 7C; Supplementary Fig. 3C, online only). As expected based on immunohistochemistry, the number of TUNEL$^+$ cells significantly increased in *Ddx4-Cre Rb1*^{flox/−} mice (Fig. 7D; Supplementary Fig. 3D, online only). These results suggest that prenatal loss of *Rb1 in vivo* induces DNA damage and *Trp53* activation, thereby increasing apoptosis and infertility in *Ddx4-Cre Rb1*^{flox/−} mice.

Discussion

This study was performed to increase our understanding of the G1/S transition in GS cells. We were interested in this process because we

found that loss of *Cdkn1b* decreased self-renewal division and that *Ccnd2* acts downstream of HRAS to promote self-renewal division [7, 24]. CDKN1B is known to suppress the cell cycle but also to play a critical role in forming the CDK4/6-CCND complex, whose primary target is RB1 [11]. Although *Rb1* has been implicated in SSC self-renewal, the roles of *Rb1* in SSCs remain unclear. Therefore, understanding the relationship between these molecules would provide valuable information on the mechanism of self-renewal division.

We first found that *Cdk4* is responsible for SSC activity. Although depletion of *Cdk4* or *Cdk6* suppressed GS cell proliferation, only *Cdk4* depletion showed significant effects on SSC activity. Reduced proliferation of *Cdk4*-depleted spermatogonia was consistent with the previous observation that *Cdk4* KO mice show decreased spermatogenesis and gradual loss of fertility [38]. Although SSC activity was not examined in that study, the results of our transplantation assay confirmed that *Cdk4* plays a role in SSCs. Since we previously demonstrated that self-renewal of SSCs by cytokines is mediated by *Hras* and *Ccnd2* [7], these results suggest that CDK4 combines with CCND2 to drive SSC self-renewal.

A major target of the CDK4 kinase is RB1. RB1 phosphorylation was significantly reduced by depletion of *Cdk4*, but not *Cdk6*. Our analysis further showed that *Cdkn1b* depletion not only reduced GS cell proliferation but also RB1 and its phosphorylation levels. In many cases, RB1 dephosphorylation is associated with a reduction in RB1 [39]. Although kinase inhibitory protein (KIP) OE suppresses cell progression, a low level of KIP proteins is also known to be important for formation of the CDK4-CCND complex [11]. Because the amount of CDK4 protein is diminished by *Cdkn1b* depletion, the RB1 phosphorylation level is significantly decreased by poor CDK4-CCND complex formation and reduced CDK4 levels. However, note that *Cdk4* and *Cdkn1b* may not function in a similar manner. In fact, unlike *Cdk4* KO mice that have small testes, *Cdkn1b* KO mice have enlarged testes and are fertile [40]. The possibility exists that other KIP family molecules, such as CDKN1C, are involved in RB1 phosphorylation. However, our results strongly suggest that *Cdkn1b* is one of the major drivers of cell cycle progression in SSCs.

We also showed that *Rb1* deficiency reduces colony formation after transplantation. Transfection of *E7*, which binds to RB1 and promotes its ubiquitin-mediated degradation [26], also resulted in poor colonization. These results are consistent with previous findings showing that transient depletion of *Rb1* by siRNA in primary cultures of undifferentiated spermatogonia decreases colony formation after transplantation [13]. However, a critical difference between the current study and the previous study was the colony morphology. *Rb1* depletion by siRNA produced large clumps of donor cells, and the cells were suggested to be malignant because colonies of them invaded interstitial cells. These changes occurred despite transient transfection of siRNA against *Rb1*, which suggested a strong growth inhibitory function of *Rb1*. Contrary to these observations, we did not observe apparent cancerous lesions in the current study. Although the cause of these discrepancies remains unknown, *Rb1* inhibition by siRNA in the previous study may have influenced additional off-target genes and caused tumor-like cell formation. Alternatively, the differences may have been caused by the differences in the genetic backgrounds (C57BL/6 (B6) *vs*. 129/B6). Thus, although both studies support the importance of *Rb1* in SSC self-renewal,
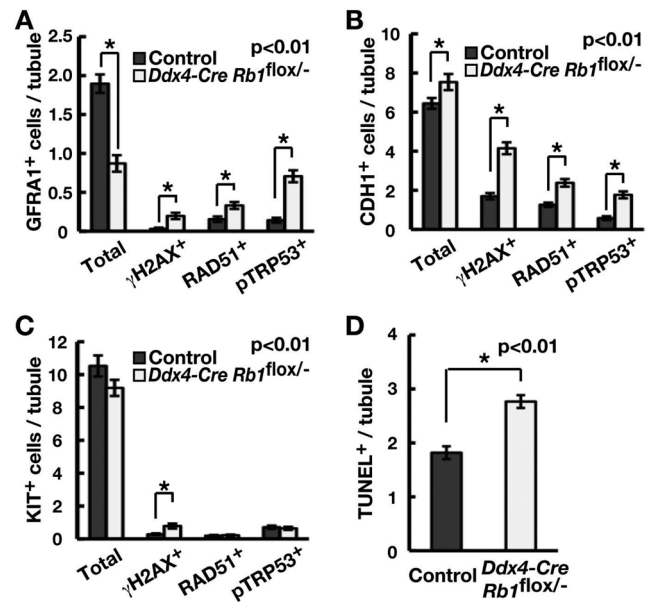
Fig. 7. Analysis of undifferentiated spermatogonia in *Ddx4-Cre Rb1*flox/– mice. (A–C) Immunohistochemical analysis of γH2AX, RAD51 or pTRP53 expression in GFRA1+ (A), CDH1+ (B) or KIT+ (C) cells in the 10-day-old *Ddx4-Cre Rb1*flox/– mouse testis. At least 50 tubules were counted in three testes. (D) TUNEL staining of the 10-day-old *Ddx4-Cre Rb1*flox/– mouse testis. At least 50 tubules were counted in three testes. Representative pictures are shown in Supplementary Fig. 3 (online only).

the reasons for these discrepancies remain unclear.

Using GS cells, we examined the mechanism of reduced SSC activity. Although we observed increased expression of *Sox3*, whether SSCs were fully committed to differentiation was not clear because other differentiating spermatogonia marker levels did not change significantly. *Rb1* deficiency induced DNA DSBs, which was confirmed based on increased expression of DNA damage proteins and a comet assay. Increased DNA damage protein expression was also found when *E2f1* was overexpressed in GS cells. Because *E2f1* depletion could decrease γH2AX expression in *Rb1* KO GS cells, we speculate that *Rb1* plays a critical role in genomic stability via regulation of E2F1. Although a direct causal relationship between RB1 and E2F1 has not been completely clarified in this study, the involvement of *E2f1* in spermatogonial proliferation was previously reported; *E2f1* deficiency results in spermatogonia depletion [30, 31], while *E2f1* OE also impairs spermatogenesis [29]. However, how these changes occur *in vivo* and whether they influence SSCs remain unclear. Our results showed that *E2f1* OE suppresses cell cycle progression by inducing DNA damage, which likely causes reduced colony formation. E2F1 stimulates DNA damage by activating DNA replication at inappropriate times [41]. Although E2F1 is known to support an apoptotic DNA damage response in *Trp53*-dependent and *Trp53*-independent pathways [42], partial rescue of *Rb1* KO cells by *Trp53* depletion suggests that DNA damage caused by the RB-E2F1 pathway activates *Trp53*. Based on these observations, we analyzed *Trp53* downstream genes to explain the *Rb1* KO GS cell phenotype.

We observed that an important characteristic of the *Rb1* KO GS cell phenotype is cell cycle arrest, which was unexpected because *Rb1* was previously shown to suppress the cell cycle progression of undifferentiated spermatogonia by increasing the expression of *Ccnd2* and *Ccne1* [13]. However, we found that GS cells upregulate *Cdkn1a* and *Cdkn2a* upon induction of *Rb1* deficiency. Although *Cdkn1a* deficiency does not influence SSC self-renewal *in vivo* [24], *Cdkn1a* OE occurs in *Atm* deficient GS cells and inhibits their proliferation [43]. However, the role of *Cdkn2a* in SSCs remains unclear because no apparent reproductive phenotype has been reported in *Cdkn2a* KO mice. When we examined the impact of these CDKIs, suppression of *Cdkn1a* (but not *Cdkn2a*) resulted in increased cell recovery, suggesting that *Cdkn1a* is responsible for cell cycle arrest upon *Rb1* deletion. Because depletion of *Trp53*, which suppresses *Cdkn1a*, also improved cell recovery, activation of the *Trp53-Cdkn1a* pathway is likely responsible for suppressing the cell cycle arrest that occurs upon induction of *Rb1* deficiency.

Increased apoptosis was another feature of *Rb1* KO GS cells. Our analysis revealed that *Bbc3* is upregulated in *Rb1* KO GS cells. *Bbc3* OE caused increased apoptosis, while its depletion increased cell survival. This increase in apoptosis may explain why we observed no apparent chromosomal abnormalities in *Rb1* KO GS cells. Genomic damage was also reported in both mouse and human embryonic stem (ES) cells that were deficient in *Rb1*. However, while we did not observe an increase in chromosome number, both mouse and human ES cells showed a high incidence of chromosomal abnormalities [44, 45]. In particular, human ES cells showed increased 4N cells, but *Cdkn1a* KD did not affect the genomic instability. Mouse ES cells may have adapted to the complete loss of function of *Rb* family members. In contrast to ES cells that often show trisomy in chromosome 8 or 11 [46, 47], GS cells are relatively stable as far as chromosomal abnormalities are concerned. We previously showed that GS cells maintain euploidy for at least 2 years [6], which is suggestive of stable genetic integrity. GS cells may be more susceptible to DNA damage, and those that have experienced severe damage may be eliminated by apoptosis instead of acquiring additional mutations before the occurrence of apparent chromosomal aberrations. Because ES cells do not show severe checkpoint responses [48], they likely easily acquire more damage, leading to increased chromosome abnormalities.

Increased DNA damage proteins in *Ddx4-Cre Rb1*^flox/– mice showed that DNA damage was caused by *Rb1* deficiency *in vivo*. Although the number of GFRA1+ spermatogonia decreased, an increased number of CDH1+ spermatogonia was observed. This result is in contrast to our observation of GS cells that showed apoptosis and blocked cell cycle progression. This difference may have occurred because *Ddx4-Cre* expression occurs prenatally at ~15.5 dpc [49]. The lack of *Rb1* during the prenatal period likely influenced the maturation of germ cells into SSCs because transplantation experiments revealed that a dramatic increase in the SSC pool size occurs postnatally [50]. A previous study showed that *Rb1* deficiency causes a delay in cell cycle arrest and increases in *Cdkn1b* and *Cdkn2b* CDKIs in gonocytes [51]. Based on these results, it is possible that the lack of cell cycle arrest in undifferentiated spermatogonia of *Ddx4-Cre Rb1*^flox/– mice is caused by the developmental defect of gonocytes that prevents them from acquiring the ability to respond to the

Trp53-induced damage response. Future experiments are required to confirm this hypothesis.

Overall, our results support the critical roles of the CDKN1B-CDK4/CCND2-RB1-E2F1 pathway in regulating SSC self-renewal (Supplementary Fig. S4, online only). Our analysis of cell cycle progression led to the identification of regulatory functions of Rb in genomic damage. Loss of *Rb1* results in activation of *Trp53*, which induces *Bbc3* and *Cdkn1a*, compromising self-renewal division. However, several questions remain to be addressed. First, the effect of *Rb1* on SSC fate commitment remains unclear. The frequency of self-renewal and differentiating division is believed to occur at the same frequency in SSCs in a steady state [52]. In *Ddx4-Cre Rb1*^flox/– mice, A_s spermatogonia exclusively differentiated into A_pr spermatogonia and did not self-renew to form new A_s spermatogonia [12]. Although we observed increased expression of *Sox3*, we were not able to obtain evidence for the role of *Rb1* in SSC differentiation. Second, the effect of E2F1 on genetic integrity has not been characterized. Although E2F1 is responsible, determining how activation of E2F1 leads to DNA damage in SSCs requires further study, and the molecular targets of E2F1 need to be identified. Finally, how E2F1 is regulated in SSCs remains unknown. Because *E2f1* deficiency leads to spermatogonia depletion in *E2f1* KO mice, the activity of E2F1 requires tight regulation to assure genetic integrity and cell cycle progression. In addition to regulation by *Rb1*, other molecules may control or modify E2F1 function, such as *Myc* and *Foxo*, which are known to influence SSCs. Thus, characterizing the molecular networks surrounding *Rb1* will increase our understanding of how SSCs determine the choice between self-renewal and differentiating divisions and how germ cells maintain genetic integrity.

References

1. **de Rooij DG, Russell LD.** All you wanted to know about spermatogonia but were afraid to ask. *J Androl* 2000; **21**: 776–798. [Medline]

2. **Meistrich ML, van Beek MEAB.** Spermatogonial stem cells. *In*: Desjardins C, Ewing LL (eds.), Cell and Molecular Biology of the Testis. New York: Oxford University Press; 1993: 266–295.

3. **Nagano M, Avarbock MR, Brinster RL.** Pattern and kinetics of mouse donor spermatogonial stem cell colonization in recipient testes. *Biol Reprod* 1999; **60**: 1429–1436. [Medline] [CrossRef]

4. **Ogawa T, Ohmura M, Yumura Y, Sawada H, Kubota Y.** Expansion of murine spermatogonial stem cells through serial transplantation. *Biol Reprod* 2003; **68**: 316–322. [Medline] [CrossRef]

5. **Kanatsu-Shinohara M, Ogonuki N, Inoue K, Miki H, Ogura A, Toyokuni S, Shinohara T.** Long-term proliferation in culture and germline transmission of mouse male germline stem cells. *Biol Reprod* 2003; **69**: 612–616. [Medline] [CrossRef]

6. **Kanatsu-Shinohara M, Ogonuki N, Iwano T, Lee J, Kazuki Y, Inoue K, Miki H, Takehashi M, Toyokuni S, Shinkai Y, Oshimura M, Ishino F, Ogura A, Shinohara T.** Genetic and epigenetic properties of mouse male germline stem cells during long-term culture. *Development* 2005; **132**: 4155–4163. [Medline] [CrossRef]

7. **Lee J, Kanatsu-Shinohara M, Morimoto H, Kazuki Y, Takashima S, Oshimura M, Toyokuni S, Shinohara T.** Genetic reconstruction of mouse spermatogonial stem cell self-renewal in vitro by Ras-cyclin D2 activation. *Cell Stem Cell* 2009; **5**: 76–86. [Medline] [CrossRef]

8. **Oatley JM, Avarbock MR, Brinster RL.** Glial cell line-derived neurotrophic factor regulation of genes essential for self-renewal of mouse spermatogonial stem cells is dependent on Src family kinase signaling. *J Biol Chem* 2007; **282**: 25842–25851. [Medline]

[CrossRef]

9. **Bartkova J, Rajpert-De Meyts E, Skakkebaek NE, Lukas J, Bartek J.** Deregulation of the G1/S-phase control in human testicular germ cell tumours. *APMIS* 2003; **111**: 252–265, discussion :265–266. [Medline] [CrossRef]

10. **Goriely A, Hansen RM, Taylor IB, Olesen IA, Jacobsen GK, McGowan SJ, Pfeifer SP, McVean GA, Rajpert-De Meyts E, Wilkie AO.** Activating mutations in FGFR3 and HRAS reveal a shared genetic origin for congenital disorders and testicular tumors. *Nat Genet* 2009; **41**: 1247–1252. [Medline] [CrossRef]

11. **Weinberg RA.** pRB and control of the cell cycle clock. *In*: Weinberg RA (ed.), The Biology of Cancer. New York: Garland Science; 2007: 255–306.

12. **Hu YC, de Rooij DG, Page DC.** Tumor suppressor gene *Rb* is required for self-renewal of spermatogonial stem cells in mice. *Proc Natl Acad Sci USA* 2013; **110**: 12685–12690. [Medline] [CrossRef]

13. **Yang QE, Gwost I, Oatley MJ, Oatley JM.** Retinoblastoma protein (RB1) controls fate determination in stem cells and progenitors of the mouse male germline. *Biol Reprod* 2013; **89**: 113. [Medline] [CrossRef]

14. **Marino S, Vooijs M, van Der Gulden H, Jonkers J, Berns A.** Induction of medulloblastomas in p53-null mutant mice by somatic inactivation of Rb in the external granular layer cells of the cerebellum. *Genes Dev* 2000; **14**: 994–1004. [Medline]

15. **Soriano P.** Generalized lacZ expression with the ROSA26 Cre reporter strain. *Nat Genet* 1999; **21**: 70–71. [Medline] [CrossRef]

16. **Takehashi M, Kanatsu-Shinohara M, Inoue K, Ogonuki N, Miki H, Toyokuni S, Ogura A, Shinohara T.** Adenovirus-mediated gene delivery into mouse spermatogonial stem cells. *Proc Natl Acad Sci USA* 2007; **104**: 2596–2601. [Medline] [CrossRef]

17. **Ogawa T, Aréchaga JM, Avarbock MR, Brinster RL.** Transplantation of testis germinal cells into mouse seminiferous tubules. *Int J Dev Biol* 1997; **41**: 111–122. [Medline]

18. **Kanatsu-Shinohara M, Ogonuki N, Inoue K, Ogura A, Toyokuni S, Honjo T, Shinohara T.** Allogeneic offspring produced by male germ line stem cell transplantation into infertile mouse testis. *Biol Reprod* 2003; **68**: 167–173. [Medline] [CrossRef]

19. **Kanatsu-Shinohara M, Inoue K, Ogonuki N, Morimoto H, Ogura A, Shinohara T.** Serum- and feeder-free culture of mouse germline stem cells. *Biol Reprod* 2011; **84**: 97–105. [Medline] [CrossRef]

20. **Kanatsu-Shinohara M, Inoue K, Lee J, Yoshimoto M, Ogonuki N, Miki H, Baba S, Kato T, Kazuki Y, Toyokuni S, Toyoshima M, Niwa O, Oshimura M, Heike T, Nakahata T, Ishino F, Ogura A, Shinohara T.** Generation of pluripotent stem cells from neonatal mouse testis. *Cell* 2004; **119**: 1001–1012. [Medline] [CrossRef]

21. **Kanatsu-Shinohara M, Muneto T, Lee J, Takenaka M, Chuma S, Nakatsuji N, Horiuchi T, Shinohara T.** Long-term culture of male germline stem cells from hamster testes. *Biol Reprod* 2008; **78**: 611–617. [Medline] [CrossRef]

22. **Vooijs M, van der Valk M, te Riele H, Berns A.** Flp-mediated tissue-specific inactivation of the retinoblastoma tumor suppressor gene in the mouse. *Oncogene* 1998; **17**: 1–12. [Medline] [CrossRef]

23. **Brinster RL, Zimmermann JW.** Spermatogenesis following male germ-cell transplantation. *Proc Natl Acad Sci USA* 1994; **91**: 11298–11302. [Medline] [CrossRef]

24. **Kanatsu-Shinohara M, Takashima S, Shinohara T.** Transmission distortion by loss of p21 or p27 cyclin-dependent kinase inhibitors following competitive spermatogonial transplantation. *Proc Natl Acad Sci USA* 2010; **107**: 6210–6215. [Medline] [CrossRef]

25. **Knudsen KE, Weber E, Arden KC, Cavenee WK, Feramisco JR, Knudsen ES.** The retinoblastoma tumor suppressor inhibits cellular proliferation through two distinct mechanisms: inhibition of cell cycle progression and induction of cell death. *Oncogene* 1999; **18**: 5239–5245. [Medline] [CrossRef]

26. **Boyer SN, Wazer DE, Band V.** E7 protein of human papilloma virus-16 induces degradation of retinoblastoma protein through the ubiquitin-proteasome pathway. *Cancer Res* 1996; **56**: 4620–4624. [Medline]

27. **Sariola H, Saarma M.** Novel functions and signalling pathways for GDNF. *J Cell Sci* 2003; **116**: 3855–3862. [Medline] [CrossRef]

28. **Müller H, Helin K.** The E2F transcription factors: key regulators of cell proliferation. *Biochim Biophys Acta* 2000; **1470**: M1–M12. [Medline]

29. **Agger K, Santoni-Rugiu E, Holmberg C, Karlström O, Helin K.** Conditional E2F1 activation in transgenic mice causes testicular atrophy and dysplasia mimicking human CIS. *Oncogene* 2005; **24**: 780–789. [Medline] [CrossRef]

30. **Hoja MR, Liu JG, Mohammadieh M, Kvist U, Yuan L.** E2F1 deficiency impairs murine spermatogenesis and augments testicular degeneration in SCP3-nullizygous mice.

Cell Death Differ 2004; **11**: 354–356. [Medline] [CrossRef]

31. **Yamasaki L, Jacks T, Bronson R, Goillot E, Harlow E, Dyson NJ.** Tumor induction and tissue atrophy in mice lacking E2F-1. *Cell* 1996; **85**: 537–548. [Medline] [CrossRef]

32. **Pützer BM, Engelmann D.** E2F1 apoptosis counterattacked: evil strikes back. *Trends Mol Med* 2013; **19**: 89–98. [Medline] [CrossRef]

33. **Oda K, Arakawa H, Tanaka T, Matsuda K, Tanikawa C, Mori T, Nishimori H, Tamai K, Tokino T, Nakamura Y, Taya Y.** p53AIP1, a potential mediator of p53-dependent apoptosis, and its regulation by Ser-46-phosphorylated p53. *Cell* 2000; **102**: 849–862. [Medline] [CrossRef]

34. **Wu Z, Earle J, Saito S, Anderson CW, Appella E, Xu Y.** Mutation of mouse p53 Ser23 and the response to DNA damage. *Mol Cell Biol* 2002; **22**: 2441–2449. [Medline] [CrossRef]

35. **Meuwissen R, Linn SC, Linnoila RI, Zevenhoven J, Mooi WJ, Berns A.** Induction of small cell lung cancer by somatic inactivation of both Trp53 and Rb1 in a conditional mouse model. *Cancer Cell* 2003; **4**: 181–189. [Medline] [CrossRef]

36. **Grisanti L, Falciatori I, Grasso M, Dovere L, Fera S, Muciaccia B, Fuso A, Berno V, Boitani C, Stefanini M, Vicini E.** Identification of spermatogonial stem cell subsets by morphological analysis and prospective isolation. *Stem Cells* 2009; **27**: 3043–3052. [Medline]

37. **Tokuda M, Kadokawa Y, Kurahashi H, Marunouchi T.** CDH1 is a specific marker for undifferentiated spermatogonia in mouse testes. *Biol Reprod* 2007; **76**: 130–141. [Medline] [CrossRef]

38. **Rane SG, Dubus P, Mettus RV, Galbreath EJ, Boden G, Reddy EP, Barbacid M.** Loss of Cdk4 expression causes insulin-deficient diabetes and Cdk4 activation results in beta-islet cell hyperplasia. *Nat Genet* 1999; **22**: 44–52. [Medline] [CrossRef]

39. **Broude EV, Swift ME, Vivo C, Chang BD, Davis BM, Kalurupalle S, Blagosklonny MV, Roninson IB.** p21(Waf1/Cip1/Sdi1) mediates retinoblastoma protein degradation. *Oncogene* 2007; **26**: 6954–6958. [Medline] [CrossRef]

40. **Beumer TL, Kiyokawa H, Roepers-Gajadien HL, van den Bos LA, Lock TM, Gademan IS, Rutgers DH, Koff A, de Rooij DG.** Regulatory role of p27kip1 in the mouse and human testis. *Endocrinology* 1999; **140**: 1834–1840. [Medline] [CrossRef]

41. **Pickering MT, Kowalik TF.** Rb inactivation leads to E2F1-mediated DNA double-strand break accumulation. *Oncogene* 2006; **25**: 746–755. [Medline] [CrossRef]

42. **Croxton R, Ma Y, Song L, Haura EB, Cress WD.** Direct repression of the Mcl-1 promoter by E2F1. *Oncogene* 2002; **21**: 1359–1369. [Medline] [CrossRef]

43. **Takubo K, Ohmura M, Azuma M, Nagamatsu G, Yamada W, Arai F, Hirao A, Suda T.** Stem cell defects in ATM-deficient undifferentiated spermatogonia through DNA damage-induced cell-cycle arrest. *Cell Stem Cell* 2008; **2**: 170–182. [Medline] [CrossRef]

44. **Conklin JF, Baker J, Sage J.** The RB family is required for the self-renewal and survival of human embryonic stem cells. *Nat Commun* 2012; **3**: 1244. [Medline] [CrossRef]

45. **Zheng L, Flesken-Nikitin A, Chen PL, Lee WH.** Deficiency of Retinoblastoma gene in mouse embryonic stem cells leads to genetic instability. *Cancer Res* 2002; **62**: 2498–2502. [Medline]

46. **Liu X, Wu H, Loring J, Hormuzdi S, Disteche CM, Bornstein P, Jaenisch R.** Trisomy eight in ES cells is a common potential problem in gene targeting and interferes with germ line transmission. *Dev Dyn* 1997; **209**: 85–91. [Medline] [CrossRef]

47. **Longo L, Bygrave A, Grosveld FG, Pandolfi PP.** The chromosome make-up of mouse embryonic stem cells is predictive of somatic and germ cell chimaerism. *Transgenic Res* 1997; **6**: 321–328. [Medline] [CrossRef]

48. **Aladjem MI, Spike BT, Rodewald LW, Hope TJ, Klemm M, Jaenisch R, Wahl GM.** ES cells do not activate p53-dependent stress responses and undergo p53-independent apoptosis in response to DNA damage. *Curr Biol* 1998; **8**: 145–155. [Medline] [CrossRef]

49. **Gallardo T, Shirley L, John GB, Castrillon DH.** Generation of a germ cell-specific mouse transgenic Cre line, Vasa-Cre. *Genesis* 2007; **45**: 413–417. [Medline] [CrossRef]

50. **Shinohara T, Orwig KE, Avarbock MR, Brinster RL.** Remodeling of the postnatal mouse testis is accompanied by dramatic changes in stem cell number and niche accessibility. *Proc Natl Acad Sci USA* 2001; **98**: 6186–6191. [Medline] [CrossRef]

51. **Spiller CM, Wilhelm D, Koopman P.** Retinoblastoma 1 protein modulates XY germ cell entry into G1/G0 arrest during fetal development in mice. *Biol Reprod* 2010; **82**: 433–443. [Medline] [CrossRef]

52. **de Rooij DG.** Proliferation and differentiation of spermatogonial stem cells. *Reproduction* 2001; **121**: 347–354. [Medline] [CrossRef]